JOURNAL OF NANO AND MATERIALS SCIENCE RESEARCH
Volume 3, No.2 (Special Issue, 2025), pp. 21 – 27
Available online at journals.nanotechunn.com/jnmsr

ORIGINAL ARTICLE

Development of Chalcogenide Sb_2Se_3 Thin Film by Simple and Low-Cost Chemical Bath Deposition Technique for Optoelectronics Applications

J. A. Ezihe [a,b,*], *M. Abdulwahab* [a,c], *F. I. Ezema* [a,d], *O. K. Echendu* [a,b]

[a]*Africa Centre of Excellence in Future Energies and Electrochemical systems, Federal University of Technology, P.M.B. 1526, Owerri, Nigeria*
[b]*Department of Physics, Federal University of Technology, P.M.B. 1526, Owerri, Nigeria*
[c]*Metallurgical and Materials Engineering Department, Air Force Institute of Technology, Nigeria Air Force, P.M.B. 2104, Kaduna, Nigeria*
[d]*Department of Physics and Astronomy, University of Nigeria Nsukka, 410001 Nsukka, Nigeria*

KEYWORDS

Selenosulphate,
Reflux,
Solar cell,
Photodetector,
Amorphous

ARTICLE HISTORY

Received: May 11, 2025
Revised: May 25, 2025
Accepted: June 06, 2024
Published: June 16, 2025

ABSTRACT

Antimony selenide (Sb_2Se_3) thin films were synthesized for potential application in optoelectronic devices using a low-cost, facile chemical bath deposition (CBD) technique. The as-deposited films exhibit a characteristic brown coloration, indicative of phase formation. The selenium precursor, sodium selenosulfate (Na_2SeSO_3), was synthesized via a reflux process involving elemental selenium and sodium sulphite ($NaSO_3$), ensuring a controlled release of Se^{2-} ions during deposition. The materials were characterized for structural, optical, morphological and compositional properties. X-ray diffraction (XRD) measurement revealed amorphous nature of the film's material for as-synthesized films as well as films annealed at 100 ℃ and 150 ℃ in the absence of selenium environment. The optical property showed that the material has capacity for high absorption in the UV and visible regions of the solar spectrum as indicated by low transmittance in these regions. The indirect bandgap was estimated to be 1.12 eV for as-deposited material, 1.01 eV for 100 ℃ annealed film and 0.90 eV for 150 ℃ annealed sample. RMS roughness decreases uniformly with increase in annealing temperature as indicated by Atomic Force Microscopy (AFM) measurement. Scanning Electron Microscopy (SEM) confirmed the uniformity in the surface morphology of the material. Energy dispersive X-ray fluorescence spectroscopy (EDXRF) confirmed the presence of Sb and Se in the material. The high absorption in the visible and UV regions makes the material a good candidate for solar cell absorption layer and photodetectors.

1 Introduction

Over the past four decades, Sb_2Se_3 has garnered significant attention owing to its remarkable material properties. Its appeal lies in its single stable crystalline phase, high optical absorption coefficient, favourable direct–indirect bandgap characteristics, efficient hole mobility, and a unique layered crystal structure characterized by weak van der Waals interlayer interactions and the absence of dangling bonds [1].

Sb_2Se_3 gained significant attention from researchers due to its favourable band gap (1–1.3 eV), high optical absorption coefficient (more than 10^5 cm^{-1} at visible light), high carrier mobility (approximately 10 $cm^2V^{-1}s^{-1}$), and cost-effectiveness [2]–[8].

Currently, Sb_2Se_3-based thin-film solar cells exhibited efficiency values of 10% [9]–[11]. However, according to the ideal Shockley-Queisser limit, their theoretical efficiency could surpass 31% [12].

* **CORRESPONDING AUTHOR** | J. A. Ezihe, ✉ james.ezihe@futo.edu.ng

The performance of Sb_2Se_3 solar cells is strongly influenced by the method used for their fabrication. Unlike many other semiconductors that require expensive vacuum-based fabrication, Sb_2Se_3 can be deposited using a range of chemical techniques, with chemical bath deposition (CBD) offering a particularly attractive combination of simplicity, scalability, and low processing temperature [13].

In contrast to traditional absorber materials, Sb_2Se_3 features a distinctive quasi one-dimensional structure made up of $[Sb_4Se_6]_n$ ribbons [14]. These ribbons are connected through van der Waals interactions, lacking any dangling bonds, while the atoms (Sb-Se) within each ribbon are covalently bonded [14]–[17]. As a result, Sb_2Se_3 exhibits anisotropic characteristics, with its electrical, magnetic, and optical properties varying based on the direction of its crystal growth [18].

Based on its electrochemical characteristics, Sb_2Se_3 has been proposed as a potential anode material for lithium-ion batteries [19]. In photoelectrochemical water splitting devices Sb_2Se_3 has shown promising results [20]. Additionally, this binary compound has found applications in optical recording materials [21], thermoelectric devices [22], as well as in solar cells [23].

In this study, Sb_2Se_3 thin films were synthesized via a chemical bath deposition (CBD) technique, employing Na_2SeSO_3 as the selenium source. The Na_2SeSO_3 precursor was prepared through a controlled reflux reaction involving elemental selenium powder and Na_2SO_3. Despite the potential advantages of the CBD route, there are limited reports in the literature on its application for the deposition of Sb_2Se_3 thin films. This deposition method offers significant advantages, including low cost, simplicity, high reproducibility, and scalability, rendering it a promising candidate for the large-scale fabrication of Sb_2Se_3-based photovoltaic devices.

2 Experimental Methods

The synthesis of Sb_2Se_3 is facilitated using the following chemical precursors and complexing agents: Na_2SeSO_3 serves as the selenium (Se) source, antimony trichloride ($SbCl_3$) (sigma-Aldrich, ≥ 99%) acts as the antimony (Sb) precursor, while sodium citrate (Fisher BioReagents ≥ 99%) and ammonia (JHD 30%) are employed as complexing agents to stabilize the reaction solution.

Na_2SeSO_3 was produced by refluxing via heating 8 grams of selenium powder (Aldrich, 99.9%) and 25 grams of sodium sulphite (sigma-Aldrich, ≥ 98%) in 200 ml of deionized water for four hours at a temperature of 90 ℃. This procedure is aimed at enhancing the reaction efficiency and yield. The chemical reaction is given by Equation 1:

$$Na_2SO_3 + Se \leftrightharpoons Na_2SeSO_3 \quad (1)$$

After the mixture cooled to room temperature, unreacted selenium was filtered out. The resulting sodium selenosulfate solution was subsequently placed in a dark bottle to shield it from light, which helps maintain its stability and prevents degradation. This precaution is essential for preserving the compound's integrity for future applications or analysis.

Due to its simplicity, reproducibility, low cost, and scalability, the chemical bath deposition method [24] was employed to grow high-quality Sb_2Se_3 semiconductor thin films on glass substrates. The deposition setup is shown in Figure 1.

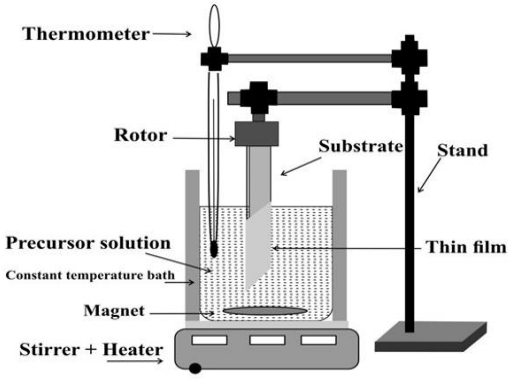

Figure 1: Set-up for chemical bath deposition of Sb_2Se_3 thin film

0.8 g of $SbCl_3$ was dissolved in 3.0 ml of acetone and stirred for 2 minutes. And this was followed by the addition of 36 ml of 1 M sodium citrate with stirring, then 20 ml of ammonia was added with continuous stirring and then 24 ml of sodium selenosulfate was added to the solution and stirred for 2 minutes, and de-ionized water took the volume to 100 ml. The bath was maintained at 50° for 65 minutes.

The film growth process is represented as follows:

The formation of antimony (III) citrate complex is represented by Equation 2:

$$SbCl_3 + Na_3C_6H_5O_7 \rightarrow Sb(C_6H_5O_7) + 3NaCl \quad (2)$$

Antimony ion is released from antimony (III) citrate complex,

$$Sb(C_6H_5O_7) \rightleftharpoons Sb^{3+} + C_6H_5O_7^{3-} \quad (3)$$

Then hydrolysis of sodium selenosulfate releases Se^{2-}:

$$Na_2SeSO_3 + 2OH^- \rightleftharpoons Se^{2-} + Na_2SO_4 + H_2O \quad (4)$$

Then $Sb^{3+}$and Se^{2-} moved to the surface of the glass micro-slide where they were deposited as Sb_2Se_3:

$$2Sb^{3+} + 3Se^{2-} \rightleftharpoons Sb_2Se_3(s) \quad (5)$$

The slides were removed, rinsed in distilled water and dried in air. The as-deposited thin films were brown in colour and were kept in slide boxes. The samples were later annealed in air at temperatures of 100 ℃ and 150 ℃ after which they were characterized.

The brownish Sb_2Se_3 thin films were subjected to comprehensive characterization to evaluate their structural, optical, compositional, and morphological properties.

Crystallographic analysis was conducted using an XRD-6000 diffractometer (Shimadzu Co., Japan) with Cu-Kα radiation (λ = 1.5406 Å). Optical properties, including absorbance and reflectance spectra in the 200–1100 nm wavelength range, were recorded using a PerkinElmer UV-Vis-NIR spectrophotometer. Elemental composition was assessed via Energy Dispersive X-ray Fluorescence (EDXRF) using instrumentation from Thermo Fisher Scientific. Surface topography was examined utilizing a Stromlingo DIY Atomic Force Microscope (AFM). Surface morphology was further investigated with a Thermo Scientific Axia ChemiSEM (2023 model, USA).

3 Results and Discussions

There is no diffraction peaks observed from the XRD plot for as-deposited Sb_2Se_3 film and sample annealed at 150 °C under air without selenization indicating that the films are in an amorphous state as shown in Figure 2a. After annealing at 150 °C under air without selenization, the film material remained amorphous. There have been literature reports of similar results of Sb_2Se_3 thin film materials [25]–[27]. A broad shallow hump is observed at the lower angle; this is due to the glass nature of the material and glass substrate [27].

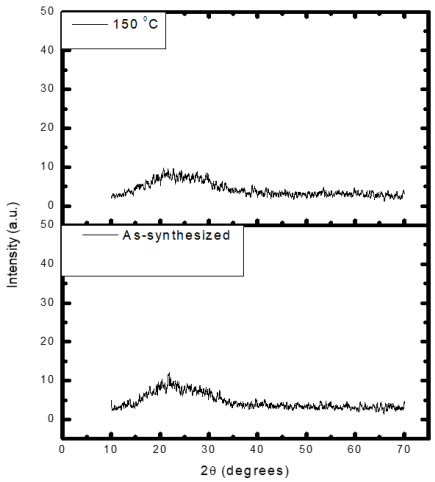

(a)

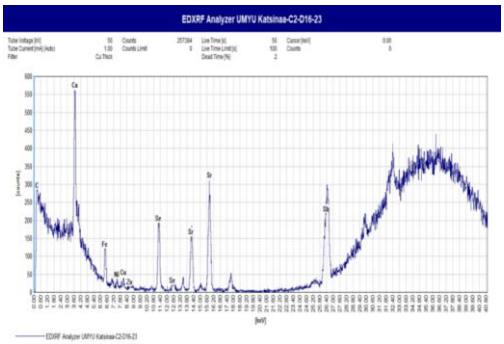

(b)

Figure 2: (a) XRD images of as-deposited and annealed Sb_2Se_3 thin film at 150 °C (b) EDXRF of Sb_2Se_3 thin film material

The compositional study was done with energy dispersive x-ray fluorescence (EDXRF), which confirmed the presence of Sb and Se in the Sb_2Se_3 film material Figure 2b. From the figure, Sb has a count of about 300 and Se has a count of 200, but the expected ratio of Sb:Se is 2:3 or Se/Sb is 1.5. The ratio of Se/Sb from the count is 0.67 which is lesser than the expected ratio of 1.5 showing that there is lower concentration of Se during production of the film material, this could be due to high volatility of Se caused by substrate temperature.

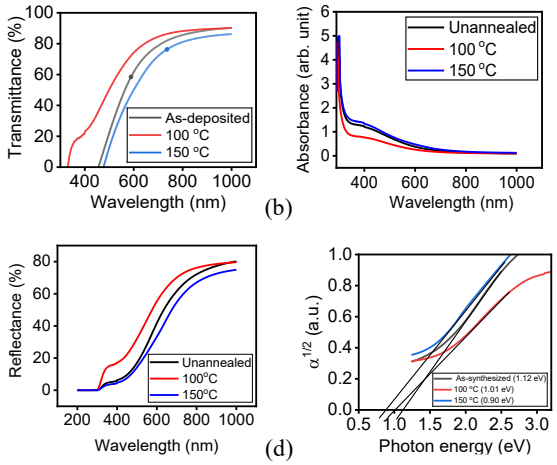

(a) (b) (c) (d)

Figure 3: (a) A graph of optical transmittance against wavelength for as-deposited and annealed Sb_2Se_3 thin film materials (b) a plot of optical absorbance against wavelength for as-deposited and annealed Sb_2Se_3 thin film materials (c) a graph of optical reflectance against wavelength for as-deposited and annealed Sb_2Se_3 thin film materials (d) a graph of indirect energy bandgap Vs photon energy for as-deposited and annealed Sb_2Se_3 thin film materials.

A graph of optical transmittance against wavelength for the as-deposited and annealed Sb_2Se_3 thin film materials is shown in Figure 3a. From the plot the material shows zero transmittance thus high absorption at low wavelengths of $\lambda < 500$ nm. After the absorption edge the transmittance rose indicating decrease in absorbance towards the near infrared region of the spectrum.

Figure 3b presents a plot of optical absorbance against wavelength for as-deposited and annealed Sb_2Se_3 thin film materials. The absorbance for both annealed and as-deposited samples steadily decreased from UV to visible and maintained a relatively constant value down to near infrared region of the spectrum. The 150 °C film exhibited the best absorbance with a value of 50 %, followed by 100 °C film with a value of about 45% and finally the as-deposited film with about the same value as 100 °C grown film in the UV region of the spectrum.

As shown in Figure 3c is a plot of optical reflectance against wavelength for as-deposited and annealed Sb_2Se_3 thin film materials. The reflectance rises from the infrared into the visible with a value of 78 % for as-synthesized as well as 100 °C films and 65 % for 150 °C film. The reflectance maintained this relatively high value into the UV region of the spectrum for the three films.

Indirect energy bandgap was confirmed by the graph of $\alpha^{1/2}$ vs photon energy for as-deposited and annealed Sb_2Se_3 thin film materials given in Figure 3d. This method has been reported by several literatures [28]–[30].

From the plot the un-annealed sample was estimated with a value of 1.12 eV, followed by the 100 ℃ grown film with a value of 1.01 eV and finally 150 ℃ sample with a value of 0.90 eV. These values agree with reported values for indirect bandgaps 1.10 to 1.85 eV by [31]–[34]. The variation in energy bandgap can be linked to the deposition method and the presence of grain boundaries. Specifically, factors such as temperature, film thickness, crystallinity, grain size, and defect states influence the band gap [35]. Elevated temperatures enhance the growth and quality of Sb_2Se_3 by increasing grain size and reducing defect states.

Post deposition annealing reduces the bandgap of the film materials; this reduction may be attributed to increase in particle size due to quantum confinement [36]. The materials have a suitable bandgap for absorption of photon energy right from the infrared region of the solar spectrum.

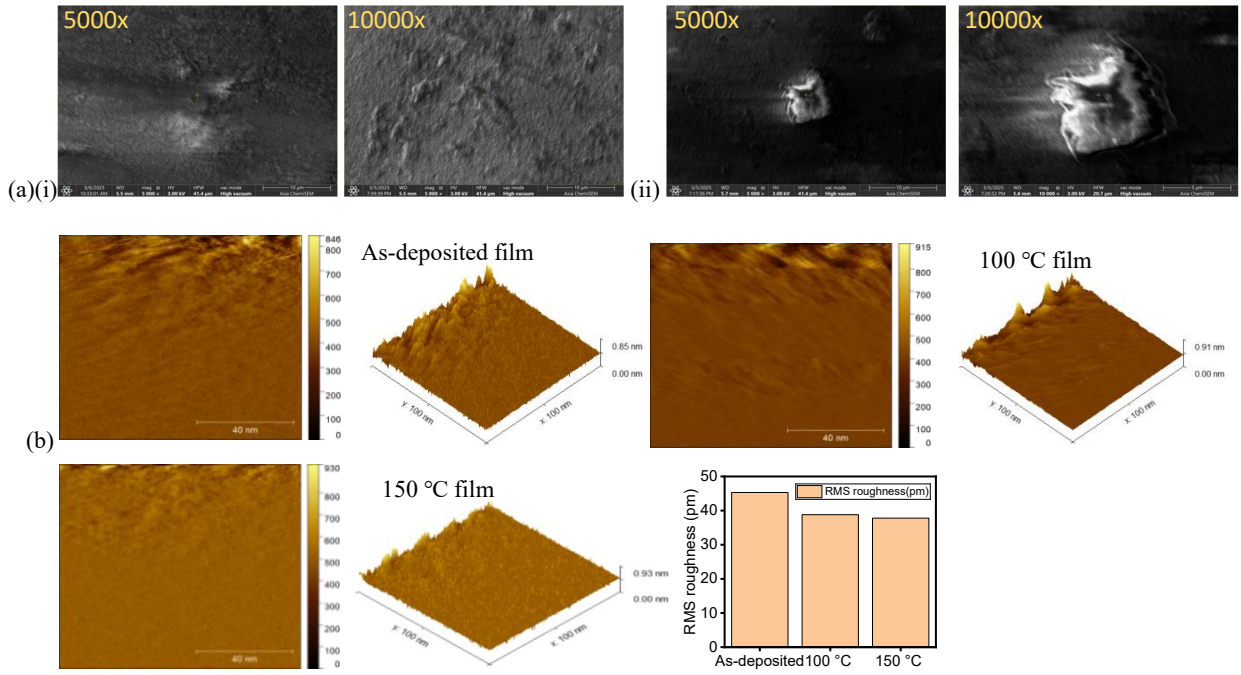

Figure 4: (a) SEM image of different magnifications of (i.) as-deposited Sb_2Se_3 thin film materials ii. annealed Sb_2Se_3 thin film materials (b) Two and three dimensions of the AFM images of as-deposited and annealed Sb_2Se_3 thin film materials (c) Bar chart of RMS roughness of AFM images of as-deposited and annealed Sb_2Se_3 thin film.

Scanning electron microscopy (SEM) images of different magnifications of (i) as-deposited Sb_2Se_3 thin film materials, and (ii) annealed Sb_2Se_3 thin film material are presented in Figure 4a. From the micrographs, it is obvious that as-synthesized films are smooth without cracks indicating amorphous nature of the films; this was evidenced by the XRD results of these samples. Annealed films showed similar trends except for the formation of artefacts which may be caused by particles from the oven.

To further analyze the morphology of the materials, we carried out atomic force microscopy (AFM) study of the thin film. Figure 4b presents the two and three dimensions of the AFM images of as-synthesized and annealed Sb_2Se_3 thin film materials depicted in Figure 4b. The film images of the samples became smoother with higher temperatures. Also bar chart of root mean square (RMS) roughness of AFM images of as-deposited and annealed Sb_2Se_3 thin film materials buttressed this fact as shown in Figure 4c. From the chart, the RMS roughness decreases uniformly with an increase in temperature, i.e. the surface becomes finer as annealing temperature increases, and grain sizes reduces. As-synthesized sample has RMS roughness value of 45.3 pm which decreases to 38.8 pm for 100 ℃ film material. With a higher temperature of 150 ℃ the roughness reduced to 37.8 pm.

Sb_2Se_3 thin-film solar cells are currently less efficient compared to commercialized technologies like CdTe and CIGS [37]; however, they present notable advantages that make them attractive for future photovoltaic applications. One of their key strengths lies in their reduced environmental impact, as Sb_2Se_3 does not rely on toxic or scarce elements. Additionally, the materials used in these cells are more abundant and potentially more cost-effective, contributing to better long-term sustainability.

These solar cells also exhibit good long-term thermal and chemical stability, which is essential for maintaining

performance over time. As a result, intensive research efforts are underway to improve their power conversion efficiency and develop scalable fabrication methods. With continued technological advancements, Sb_2Se_3 is increasingly recognized as a strong contender in the pursuit of next-generation, eco-friendly solar energy solutions.

4 Conclusions

In this work, Sb_2Se_3 thin films were synthesized via the chemical bath deposition (CBD) technique, and the influence of post-deposition annealing temperature on their morphological, structural, and optical characteristics was systematically examined, targeting their potential use as absorber layers in photovoltaic devices. X-ray diffraction (XRD) analysis indicated that the films remained amorphous in their as-deposited state as well as after annealing at 100 °C and 150 °C in the absence of selenization. Optical measurements confirmed strong absorption in both the ultraviolet (UV) and visible regions of the solar spectrum. The material exhibited an indirect optical bandgap, which progressively decreased with annealing: 1.12 eV for the as-grown film, 1.01 eV post-annealing at 100 °C, and 0.90 eV after annealing at 150 °C. Atomic force microscopy (AFM) showed a consistent decrease in root mean square (RMS) surface roughness with rising annealing temperature, while scanning electron microscopy (SEM) supported the amorphous structure. Energy dispersive X-ray fluorescence (EDXRF) analysis confirmed the presence of antimony (Sb) and selenium (Se) in the composition. The strong absorption in both UV and visible regions highlights the material's potential for use in solar cell absorber layers and photodetectors.

Acknowledgment

We appreciate our colleagues for their support and assistance.

Authors' Credit Statement

J. A. Ezihe: Experimental Design, Material Synthesis, Result analysis, Writing Original draft **M. Abdulwahab:** Supervision, **F. I. Ezema:** Experimental Design, Result Analysis, Manuscript Writing, **O. K. Echendu:** Experimental Design, Result Analysis, Manuscript Writing.

Declaration of Competing Interest

The authors declare no known competing interest or personal relationship that could influence the work reported in this paper.

References

[1] T.M. Razykov, A. Bosio, K.M. Kouchkarov, R.R. Khurramov, M.S. Tivanov, D.S. Bayko, A. Romeo, N. Romeo, Effect of substrate temperature on structure, morphology and opticalproperties of Sb2Se3 thin films fabricated by chemical-molecular beamdeposition method from Sb and Se precursors for solar cells, Thin Solid Films 791 (2024) 140218, https://doi.org/10.1016/j.tsf.2024.140218

[2] S. Porcar, A. Lahlahi, J. G. Cuadra, S. Toca, P. Serna-Gallén, D. Fraga, T. Jawhari, X. Alcobe, L. C. Barrio, P. Vidal-Fuentes, A. Pérez-Rodríguez, J. B. Carda, Electrodeposition of Sb2Se3 solar cells on ceramic tiles, Solar Energy, 290 (2025)113377, https://doi.org/10.1016/j.solener.2025.113377.

[3] A. Amin, K. Zhao, K. Khawaja, Y. Wang, D. V. Pillai, Y. Zheng, L. Li, X. Qian, F. Yan, Rapid Thermal Selenization Enhanced Efficiency in Sb2Se3 Thin Film Solar Cells with Superstrate Configuration, ACS Applied Materials & Interfaces, 17, 9 (2025) 13814-13823, DOI: 10.1021/acsami.4c19606

[4] P. Prajapat, P. Vashishtha, P. Goswami, G. Gupta, Fabrication of Sb2Se3-based high-performance self-powered Visible-NIR broadband photodetector, Materials Science in Semiconductor Processing,169 (2024)107873, https://doi.org/10.1016/j.mssp.2023.107873

[5] Y. Zhou, L. W.S. Song, J. Tang, 2017. 6.5% certified efficiency Sb2Se3 solar cells using PbS colloidal quantum dot film as hole-transporting layer. ACS. Energy Lett., 2 (9) 2125e2132ang

[6] M.A. Bilya, A. Nabok, Y.P. Purandare, A.E. Alam, I.M. Dharmadasa, Growth and Characterization of p-Type and n-Type Sb2Se3 for use in Thin-Film Photovoltaic Solar Cell Devices, energies 17 (2024) 406. https:// doi.org/10.3390/en17020406

[7] S. Porcar, A. Lahlahi, J. G. Cuadra, S. Toca, P. Serna-Gallén, D. Fraga, T. Jawhari, X. Alcobe, L. C. Barrio, P. Vidal-Fuentes, A. Pérez-Rodríguez, J. B. Carda, Electrodeposition of Sb2Se3 solar cells on ceramic tiles, Solar Energy, 290, (2025)113377, https://doi.org/10.1016/j.solener.2025.113377.

[8] R. Jakomin, S. Rampino, G. Spaggiari, M. Casappa, G. Trevisi, E. Del Canale, E. Gombia, M. Bronzoni, K.K. Sossoe, F. Mezzadri, et al. Cu-Doped Sb2Se3 Thin-Film Solar Cells Based on Hybrid Pulsed Electron Deposition/Radio Frequency Magnetron Sputtering Growth Techniques, Solar 4 (2024) 83-98. https://doi.org/10.3390/solar4010004

[9] Z. Duan, X. Liang, Y. Feng, H. Ma, B. Liang, Y. Wang, S. Luo, S. Wang, R.E.I. Schropp, Y. Mai, Z. Li, 2022. Sb2Se3 Thin Film Solar Cells Exceeding 10% Power Conversion Efficiency Enabled by Injection Vapor Deposition (IVD) Technology, Advanced Materials, 34. 10.1002/adma.202202969.

[10] Y. Zhao, S. Wang, C. Li, B. Che, X. Chen, H. Chen, R. Tang, X. Wang, G. Chen, T. Wang, et al., Regulating Deposition Kinetics via a Novel Additive-Assisted Chemical Bath Deposition Technology Enables Fabrication of 10.57%-Efficiency Sb2Se3 Solar

Cells. Energy Environ. Sci., 15 (2022) 5118–5128. https://doi.org/10.3390/en16196862.

[11] X. Xiong, C. Ding, B. Jiang, G. Zeng, B. Li, An Optimization Path for Sb2(S,Se)3 Solar Cells to Achieve an Efficiency Exceeding 20%, Nanomaterials , 14, (2024)1433. https://doi.org/10.3390/nano14171433

[12] S. Rühle, Tabulated values of the Shockley-Queisser limit for single junction solar cells, Solar Energy 130 (2016) 139–147, https://doi.org/10.1016/j. solener.2016.02.015.

[13] G. Dai, X. Wang, S. Chen, X. Chen, B. Che, T. Chen, P. Hu, J. Li, Selenium-Rich Sb2 (S, Se) 3 Thin Films Deposited via Sequential Chemical Bath Deposition for High-Efficiency Solar Cells, Advanced Functional Materials, (2025) 2415215.

[14] P. K. Nair, M. T. S. Nair, V. M. García, O. L. Arenas, Y. Pena, A. Castillo, I. T. Ayala, O. Gomezdaza, A. Sánchez, J. Campos, H. Hu, R. Suárez and M. E. Rincón, Semiconductor Thin Films by Chemical Bath Deposition for Solar Energy Related Applications, Sol. Energy Mater. Sol. Cells, 52.3-4 (1998) 313-344. doi:10.1016/S0927-0248(97)00237-7

[15] S. Campbell, L. J. Phillips, J. D. Major, O. S. Hutter, R. Voyce, Y. Qu, N. S. Beattie, G. Zoppi, V. Barrioz, Routes to increase performance for antimony selenide solar cells using inorganic hole transport layers, Frontiers in chemistry, (2022) DOI 10.3389/fchem.2022.954588

[16] H. Lei, J. Chen, Z. Tan and G. Fang, Review of Recent Progress in Antimony Chalcogenide-Based Solar Cells: Materials and Devices, Sol. RRL, 3 (2019)1900026, https://doi.org/10.1002/solr.201900026

[17] O. S. Hutter, L. J. Phillips, K. Durose and J. D. Major,6.6% efficient antimony selenide solar cells using grain structure control and an organic contact layer, Sol. Energy Mater. Sol. Cells, 188 (2018) 177–181, https://doi.org/10.1016/j.solmat.2018.09.004

[18] N. Fleck, T.D.C. Hobson, C.N. Savory, J. Buckeridge, T.D. Veal, M.R. Correia, D.O. Scanlon, K. Durose, F. Jäckel, Identifying Raman modes of Sb2Se3and their symmetries using angle-resolved polarised Raman spectra J. Mater. Chem. A 8 (2020) 8337–44

[19] R. Chen, Y. Mao, Z. Li, F. Liu, F. Gao, Phenolic resin-derived carbon-confined strategy: Sb2Se3@C@CNTs-600 with ultra-high pseudocapacitive contribution as a superior lithium-ion battery anode, Materials Chemistry and Physics, 293 (2023) 126891, https://doi.org/10.1016/j.matchemphys.2022.126891.

[20] S. J. U. Islam, M. A. Bhat, A. Hassan, A. H. Wani, M. A. Dar, K. Majid, M. Wahid, Unlocking the Electrocatalytic Potential of Sb2Se3 for HER via Cu Doping-Induced Phase Conversion and rGO Integration, Energy & Fuels, 39 (14) (2025) 6957-6967, DOI: 10.1021/acs.energyfuels.4c06119

[21] Y. Nakane, N. Sato, H. Makinon, S. Miyaoka, Principle of laser recording mechanism by forming an alloy in the multilayer of thin metallic films, in: Proceedings of the SPIE 0529, Optical Mass Data Storage I, (1985) 76.

[22] H. Zheng, L. Tan, X.-Y. Mu, Y.-T. Dun, A.-M. Mo, X.-H. Wang, M.-M. Yang, C.-L. Wu, W. Dang, R.-D. Cong, B.-L. Liang, Y. Wang, Z.-Q. Li, X.-L. Li, Exciton properties of Sb2Se3 grown in different arrays, Journal of Alloys and Compounds, 1010 (2025) 178277. https://doi.org/10.1016/j.jallcom.2024.178277.

[23] A. Hajjiah, Analytical model for photocurrent density in linearly graded band gap Sb2Se3 solar cells, Solar Energy Materials and Solar Cells, 282 (2025) 113404. https://doi.org/10.1016/j.solmat.2025.113404.

[24] A. Kuruvilla, I. M. Francis, M. Lakshmi, Effect of selenisation on the properties of antimony selenide thin films. IOP Conf. Ser.: Mater. Sci. Eng. 872 (2020) 012151. doi:10.1088/1757-899X/872/1/012151

[25] E.A. El-Sayad, A.M. Moustafa, S.Y. Marzack, Effect of heat treatment on the structural and optical properties of amorphous Sb2Se3 and Sb2Se2S thin films. Physica B 404 (2009) 1119.

[26] Z.G. Ivanova, E. Cemoskova, V.S. Vassilev, S.V. Boychera, Thermomechanical and structural characterization of GeSe2-Sb2Se3-ZnSe glasses. Mater. Lett. 57 (2003) 1025. DOI:10.101.6/S0167-577X(02)00710-3

[27] M. Malligavathy, R.T. Ananth Kumar, Chandasree Das, S. Asokan , D. Pathinettam Padiyan, Growth and characteristics of amorphous Sb2Se3 thin films of various thicknesses for memory switching applications, Journal of Non-Crystalline Solids 429 (2015) 93–97, http://dx.doi.org/10.1016/j.jnoncrysol.2015.08.038

[28] O. K. Echendu1, S. Z. Werta1, F. B. Dejene1, A. A. Ojo, I. M. Dharmadasa, Ga doping of nanocrystalline CdS thin films by electrodeposition method for solar cell application: the influence of dopant precursor concentration, Journal of Materials Science: Materials in Electronics (2019) https://doi.org/10.1007/s10854-019-00794-3

[29] O.K. Echendu, S.Z. Werta, F.B. Dejene, Effect of Cadmium precursor on the Physico-chemical properties of electrochemically grown CdS thin films for optoelectroniccs devices application: a comparative study. Journal of Materials Science: Materials in Electronics (2019) 30:365–377. https://doi.org/10.1007/s10854-018-0301-9

[30] O.K. Echendu, S.Z. Werta, F.B. Dejene, V. Craciun, Electrochemical deposition and characterization of ZnOS thin films for photovoltaic and photocatalysis

applications, Journal of Alloys and Compounds 769 (2018) 201e209. https://doi.org/10.1016/j.jallcom.2018.07.327 0

[31] B. Che, Z. Cai, H. Xu, S. Sheng, Q. Zhao, P. Xiao, J. Yang, C. Zhu, X. Zheng, R. Tang, T. Chen, 2025. Post-deposition Treatment of Sb2Se3 Enables Defect Passivation and Increased Carrier Transport Dimension for Efficient Solar Cell Application, Angewandte Chemi, 137, 16, e202425639, https://doi.org/10.1002/ange.202425639

[32] L. Shen, D. Qin, X. Hu, S. Chen, J. Tao, Utilizing methanol as a solvent auxiliary additive for the fabrication of high-efficiency Sb2Se3 solar cells. Journal of Alloys and Compounds, (2025) 1010:177967.

[33] S. Ghosh, M. V. B. Moreira, J. C. Gonzalez, Growth and optical properties of nanocrystalline Sb2Se3 thin-films for the application in solar-cells, Solar Energy, 211 (2020) 613–621, https://doi.org/doi.org/10.1016/j.solener.2020.10.001

[34] A. Mavlonov, T. Razykov, F. Raziq, J. Gan, J. Chantana, Y. Kawano, T. Nishimura, H. Wei, A. Zakutayev, T. Minemoto, X. Zu, S. Li, L. Qiao, A review of Sb2Se3 photovoltaic absorber materials and thin-film solar cells, Sol. Energy, 201 (2020) 227–246.

[35] H. He, Y. Zhong, W. Zou, X. Zhang, J. Zhao, M. Ishaq, G. Liang, A novel Se-diffused selenization strategy to suppress bulk and interfacial defects in Sb2Se3 thin film solar cell. Surfaces and Interfaces, 1, 51 (2024) 104793

[36] K. Yang, B. Li, G. Zeng, Structural, morphological, compositional, optical and electrical properties of Sb2Se3 thin films deposited by pulsed laser deposition, Superlattices and Microstructures (2020), doi: https://doi.org/10.1016/j.spmi.2020.106618

[37] J.A. Ezihe, M. Abdulwahab, F.I. Ezema, O.K. Echendu, Essential properties, growth methods, environmental impacts, and solar cell application of antimony triselenide thin films: A review, Hybrid Advances, 10 (2025) 100505, https://doi.org/10.1016/j.hybadv.2025.100505.